Frontiers in Bioscience Landmark

Front. Biosci. (Landmark Ed) **2026**; 31(9): 51724
https://doi.org/10.31083/FBL51724

Original Research

Mechanism of the NAMPT-SIRT2-Lactate Axis in Senescence of Human Nucleus Pulposus Cells

Wensheng Zhang[1], Ling Mo[1], Haiwei Guo[1], Xibing Zhang[1], Hanwu Tang[1], Wenchao Li[1], Caijun Liu[1,*]

[1]Guangdong Research Institute for Orthopedics and Traumatology of Chinese Medicine, The Third Affiliated Hospital of Guangzhou University of Chinese Medicine, 510378 Guangzhou, Guangdong, China
*Correspondence: liucaijun2005@163.com (Caijun Liu)
Academic Editor: Sung Eun Kim
Submitted: 11 March 2026 Revised: 2 July 2026 Accepted: 6 July 2026 Published: 17 September 2026

Abstract

Background: Intervertebral disc degeneration (IDD) is a primary cause of low back pain, closely associated with the senescence of nucleus pulposus cells (NPCs). Energy metabolism disorders and lactate accumulation are observed in degenerated intervertebral discs. However, the molecular mechanism through which lactate accumulation induces IDD and its upstream regulatory factors remain unclear. **Methods:** Clinical degenerated intervertebral disc tissues were collected. Lactate content was measured using the water-soluble tetrazolium salt-8 (WST-8) method, and the expression of nicotinamide phosphoribosyltransferase (NAMPT) and sirtuin 2 (SIRT2) was analyzed by western blotting. NPCs were cultured *in vitro* and treated with lactate. Lactate levels, protein lactylation, p38 mitogen-activated protein kinase (p38-MAPK) pathway activity, and cellular senescence were assessed using lactate assay kits, western blotting, and senescence-associated β-galactosidase staining, respectively. Furthermore, small interfering RNA (siRNA) and overexpression plasmids were used to regulate NAMPT expression, combined with SIRT2 activators or inhibitors, to explore the role of the NAMPT/SIRT2 axis in regulating lactate metabolism and cellular senescence. **Results:** Lactate was detected in all four degenerated intervertebral disc tissue samples examined, with variable levels among individuals. NAMPT and SIRT2 protein expression showed similar expression patterns across these samples, suggesting a potential relationship that warrants further investigation in larger cohorts. *In vitro* experiments confirmed that lactate treatment significantly elevated global protein lactylation levels, activated the p38-MAPK pathway, and induced cellular senescence in NPCs. Knockdown of NAMPT expression reduced lactate and NAD^+ levels. Notably, treatment with a SIRT2 activator partially restored the decrease in lactate content but had no significant effect on nicotinamide adenine dinucleotide (NAD^+) levels. Overexpression of NAMPT led to lactate accumulation and cellular senescence, both of which could be antagonized by either a lactate inhibitor or a SIRT2 inhibitor. **Conclusions:** *In vitro* experiments indicate that NAMPT appears to modulate lactate metabolism in a SIRT2-dependent manner, which subsequently activates the p38-MAPK signaling pathway and contributes to nucleus pulposus cell senescence. These findings suggest a functional NAMPT/SIRT2/lactate/p38-MAPK signaling axis that may play a role in intervertebral disc degeneration. However, the clinical relevance of these observations requires validation in larger patient cohorts with appropriate normal controls. Although further *in vivo* validation and mechanistic details (e.g., direct regulation of SIRT2 activity) are required, this axis may represent a potential therapeutic target for intervening in IDD.

Keywords: intervertebral disc degeneration; nucleus pulposus; nicotinamide phosphoribosyltransferase; sirtuin 2; lactic acid

1. Introduction

Low back pain (LBP), with a prevalence of approximately a 20% and high disability rate, has become a significant public health issue [1]. Intervertebral disc degeneration (IDD) is the main pathological basis for LBP [2] and the senescence and apoptosis of nucleus pulposus cells (NPCs) are key processes driving this degeneration [3]. Senescent NPCs exhibit a catabolic phenotype, characterized by reduced synthesis of extracellular matrix (ECM) components and increased the senescence-associated secretory phenotype (SASP), thereby exacerbating local inflammatory responses and matrix destruction [4,5]. Therefore, elucidating the mechanisms of NPC senescence in IDD is crucial for developing targeted therapeutic strategies.

For a long time, lactate was commonly regarded as a mere end-product of anaerobic metabolism. With the proposal of the lactate shuttle theory, its various physiological functions in energy supply, gluconeogenesis precursor, and signal transduction have been gradually revealed [6]. As an avascular tissue, the intervertebral disc primarily relies on anaerobic glycolysis for energy, a process accompanied by substantial lactate production. Studies have shown that lactate concentration is significantly elevated in degenerated intervertebral disc tissues, and its abnormal accumulation can activate signaling pathways such as protein kinase B/nuclear factor erythroid 2-related factor 2 (Akt/Nrf2), exacerbate oxidative stress responses, and further induce senescence, apoptosis, and ECM degradation in nucleus pulposus cells [7,8]. However, the upstream regu-

latory mechanisms and specific signaling pathways through which lactate drives intervertebral disc degeneration and senescence remain to be fully elucidated and warrant further investigation.

Sirtuin 2 (SIRT2) plays a crucial regulatory role in maintaining chondrocyte and nucleus pulposus cell homeostasis [9,10]. Research shows that SIRT1 expression is significantly downregulated in chondrocytes from osteoarthritis patients, and its functional inhibition further aggravates apoptosis [11]. Concurrently, nicotinamide phosphoribosyltransferase (NAMPT), the rate-limiting enzyme in nicotinamide adenine dinucleotide (NAD^+) biosynthesis, also plays an important role in bone metabolism [12] and is abnormally elevated in osteoarthritis patients [13]. Existing studies suggest that NAMPT might rejuvenate senescent nucleus pulposus cells and the endplate cells by activating the NAD^+/SIRT1 pathway, thereby improving age-related dysfunction [14]; however, evidence also indicates that in metabolic regulation, the functional link between NAMPT and SIRT2 might be more direct. For instance, in human skeletal muscle, the loss of NAMPT and SIRT2 (but not SIRT1) leads to reduced expression and activity of glyoxalase I (GLO1) [15]. Furthermore, the NAMPT/SIRT2/Lactate Dehydrogenase A (LDHA) pathway present in granulosa cells mediates lactate production [16]. These studies suggest that NAMPT and SIRT2 might play synergistic roles in cellular senescence by regulating lactate metabolism. However, how this regulatory axis participates in lactate accumulation-driven NPC senescence requires further in-depth investigation.

In summary, to investigate the roles of NAMPT, SIRT2, and lactate in intervertebral disc degeneration and senescence, this study first examined the expression levels of lactate, NAMPT, and SIRT2 in a small set of human degenerated intervertebral disc tissue samples (n = 4) as a preliminary exploratory analysis to generate hypotheses for subsequent *in vitro* mechanistic studies. Subsequently, in cultured NPCs *in vitro*, the expression of NAMPT or SIRT2 was manipulated through cell transfection to validate the core regulatory role of the NAMPT/SIRT2 axis in lactate-mediated cellular senescence, explore the molecular mechanisms of IDD, and provide a theoretical basis for targeted interventions.

2. Materials and Methods

2.1 Reagents, Equipment, and Cells

2.1.1 Clinical Tissue Sample Collection

Inclusion criteria:

(1) All patients met the diagnostic criteria for lumbar disc herniation (LDH) according to the "Guidelines for the Diagnosis and Treatment of Lumbar Disc Herniation", as confirmed by imaging examination; common LDH symptoms include acute or chronic low back pain, radiating pain in the lower extremities, limited lumbar motion, accompanied by muscle weakness or sensory abnormalities in the innervated area of the affected nerve root; physical examination reveals positive straight leg raise test, local lumbar tenderness, significant paravertebral muscle tension, motor and/or sensory dysfunction in muscles innervated by the affected nerve root, and markedly diminished tendon reflexes.

(2) History of illness >3 months, unresponsive to conservative treatment, or with progressive condition during treatment.

(3) Single-segment lesion, accompanied by nerve root pain in the responsible segment or cauda equina syndrome, presenting with muscle paralysis or bladder symptoms.

(4) Age 18–80 years, male or female.

(5) No cognitive impairment or mental illness.

Exclusion criteria:

(1) History of other severe spinal diseases, such as spinal tumors, spinal tuberculosis, osteoporotic fractures, severe intervertebral space infection, etc.

(2) Patients with lumbar instability or spondylolisthesis.

(3) Patients with bilateral lower limb symptoms or extreme lateral disc herniation.

(4) Patients who have undergone previous spinal surgery.

(5) Patients with concomitant cardiovascular or cerebrovascular diseases.

(6) Patients with coagulation disorders and abnormal liver or kidney function.

Due to the exploratory nature of this preliminary analysis and the limited availability of healthy control disc tissues (which are rarely obtainable in the absence of a surgical indication), no normal control group was included. The four samples are presented as individual case descriptions to illustrate variability and generate hypotheses, rather than to draw statistical inferences about disease-associated changes.

2.1.2 Chemicals and Reagents

PBS buffer (PB180327, Procell, Wuhan, Hubei, China); 0.25% Trypsin-EDTA (25200072, Gibco, Waltham, MA, USA); 0.4% Trypan Blue stain (15250-061, Gibco, Waltham, MA, USA); Human Nucleus Pulposus Cell Complete Medium (PY-H085, Fuheng Biology, Shanghai, China); L-Lactic acid (L1750, Merck, Darmstadt, Hesse, Germany); Lactate Assay Kit (S0208S, Beyotime, Shanghai, China); NAD^+/NADH Assay Kit (S0175, Beyotime, Shanghai, China); siRNA and NAMPT overexpression plasmid (Beijing Maijin, Beijing, China); Lipo8000 Transfection Reagent (C0533-1.5 mL, Beyotime, Shanghai, China); RNA Extraction Kit (DP451, Tiangen, Beijing, China); FastKing cDNA Synthesis PreMix (Q712-02, Tiangen, Beijing, China); ChamQ Universal SYBR qPCR Master Mix (KR118, Vazyme, Nanjing, Jiangsu, China); Western and IP Cell Lysis Buffer (P0013, Beyotime, Shanghai, China); BCA Protein Assay Kit (BL521A, Biosharp, Guangzhou, Guangdong,

China); Anti-NAMPT antibody (1:1000, MA5-44309, Thermo Fisher, Waltham, MA, USA); Anti-SIRT2 antibody (1:1000, HY-P80320, MCE, Monmouth Junction, NJ, USA); Anti-p-p38 antibody (1:1000, 28796-1-AP, Proteintech, Rosemont, IL, USA); Anti-L-Lactyllysine antibody (1:1000, PTM-1401RM, PTMBIO, Hangzhou, Zhejiang, China); Anti-GAPDH antibody (1:10,000, 60004-1-ig, Proteintech, Rosemont, IL, USA); HRP-conjugated Goat Anti-Rabbit/Mouse IgG (H+L) (1:10,000, SA00001-2/SA00001-1, Proteintech, Rosemont, IL, USA); β-Galactosidase Staining Kit (C0602, Beyotime, Shanghai, China); Latrepirdine dihydrochloride (HY-14537, MCE, Monmouth Junction, NJ, USA) (AMPK activator); Oxamic acid sodium salt (HY-W013032A, MCE, Monmouth Junction, NJ, USA) (lactate inhibitor); AGK2 (HY-100578, MCE, Monmouth Junction, NJ, USA) (SIRT2 inhibitor). Human IL-6 (ml058097, Mlbio, Shanghai, China), Human IL-8 (ml028580, Mlbio, Shanghai, China). Instruments used included a Micro High-Speed Refrigerated Centrifuge (CF1524R, Scilogex, Rocky Hill, CT, USA), Microplate Reader (MK3, Thermo, Waltham, MA, USA), Tissue Grinder Homogenizer (TGrinderH24, Tiangen, Beijing, China), Inverted Fluorescence Microscope (NIB950-FL, NEXCOPE, Ningbo, Zhejiang, China), and CO_2 Incubator (371, Thermo, Waltham, MA, USA). P0 human nucleus pulposus cells were purchased from Fuheng Biology (Shanghai). All reagents were used within their expiry date, and related operations were performed under sterile conditions.

2.1.3 Cell Culture

Human NPCs (P0) were purchased from Fuheng Biology (Shanghai). The phenotypic characteristics and purity of cultured human NPCs were verified by immunofluorescence staining for the specific marker Collagen II to confirm their biological characteristics. Received P0 cells were placed in a CO_2 incubator (37 °C, 5% CO_2) to equilibrate for 4 h before passaging. Cells were washed with PBS buffer, digested with 0.25% trypsin for 30 seconds, and then the digestion was terminated with complete medium. After centrifugation at 300 ×g for 5 min, the supernatant was discarded, and cells were resuspended in fresh complete medium. Cells were passaged at a 1:2 ratio, seeded into T25 culture flasks, gently mixed, and placed in a CO_2 incubator (37 °C, 5% CO_2). All cell lines used in this study were tested for mycoplasma contamination with negative results.

2.2 Study on the Mechanism of the NAMPT/SIRT2 Pathway in Intervertebral Disc Degeneration

2.2.1 Cell Transfection and Grouping Treatment

To investigate the function of NAMPT, we constructed cell models with NAMPT knockdown (siNAMPT) and overexpression (oeNAMPT). Transfection was performed using Lipo8000 Transfection Reagent (Beyotime, Cat# C0533-1.5ml). For siNAMPT construction, P2 cells were seeded in 6-well plates at 3×10^5/well. When cell density reached 50–60%, the old medium was discarded, and cells were starved in serum-free medium for 2 h. The transfection mixture was prepared as follows: 2 μL siRNA was mixed with 50 μL Opti-MEM, and 6 μL Lipo8000 was mixed with 50 μL Opti-MEM and incubated at room temperature for 5 min. The two solutions were then combined, incubated for 15 min at room temperature, and added to the cells. The mixture was added to the cells, which were then placed in a CO_2 incubator for 6 h. The medium was then replaced with complete medium. Transfection continued for 48 h, with medium changed every 24 h. Cells were collected after 48 h for validation. For oeNAMPT construction, when cell density reached 50–60%, the old medium was discarded, and transfection reagent was added: 2.5 μg plasmid + 125 μL Opti-Medium mixed + 4 μL Lipo8000 mixed, incubated at RT for 5 min. Cells were placed in a CO_2 incubator for 48 h, then collected for validation. Furthermore, to investigate the effect of lactate on the p38-MAPK signaling pathway and cellular senescence, cells were divided into a blank control group, a 20 μM lactate treatment group (LA), and a combination group treated with 20 μM lactate and 100 nM AMPK activator (LA+LD) [17,18,19,20]. P2 generation cells from each group were seeded into 12-well plates at 1.5×10^5 cells/well. When density reached 60–70%, corresponding drug interventions were applied for 24 h, followed by analyses such as β-galactosidase staining.

2.2.2 Lactate Content Detection

L-lactic acid content was determined using the WST-8 method (Beyotime kit). Briefly, 50 ± 5 mg of tissue sample was weighed and homogenized in 500 μL Lactate Assay Buffer using a tissue grinder at 4 °C, followed by centrifugation at 12,000 ×g for 5 min at 4 °C. The supernatant was collected for testing. A standard curve was prepared by diluting the 1 mM L-Lactate standard, with concentrations ranging from 0 to 0.64 mM. For detection, 50 μL of sample supernatant was mixed with 50 μL of WST-8 Developing Working Solution (containing enzyme solution, substrate, and WST-8), incubated at 37 °C in the dark for 30 min, and then the absorbance was measured at 450 nm. The standard curve showed a good linear relationship ($y = 2.419x + 0.0145$, $R^2 = 0.9972$). L-Lactate concentration in samples was calculated based on the standard curve.

2.2.3 β-Galactosidase Staining

Cellular senescence was detected using a β-Galactosidase Staining Kit (Beyotime, Cat# C0602). After 24 h of drug intervention, the culture medium was aspirated, cells were washed once with PBS, and 1 mL of fixative solution was added for 15 min at room temperature. After washing three times with PBS, 1 mL of staining working solution (containing 10 μL Solution A,

Table 1. Primer sequences for genes.

Gene	Forward primer	Reverse primer
β-actin	CTGGGACGACATGGAGAAAA	AAGGAAGGCTGGAAGAGTGC
NAMPT	CCTTCGGTTCTGGTGGAGGTTTG	CAGCAACTGGGTCCTTGAAGACG

10 µL Solution B, 930 µL Solution C, and 50 µL X-Gal solution) was added to each well. Plates were sealed with parafilm, incubated overnight at 37 °C, and observed and photographed under an optical microscope (4×, 10×, 20×). For quantification, five random fields were selected per group, and the numbers of blue-stained positive senescent cells and total cells were counted using ImageJ software (version 1.53, NIH, Bethesda, Maryland, USA). The cellular senescence rate was calculated as: senescence rate (%) = (number of positive cells / total cells) × 100%.

2.2.4 Real-Time Quantitative PCR (qRT-PCR)

RNA extraction was performed using the Tiangen RNA Extraction Kit (Cat# DP451). Samples were homogenized in 350 µL Lysis Buffer, 10 µL Proteinase K was added, incubated at room temperature for 5 min, and centrifuged at 12,000 rpm, 4 °C for 5 min. The supernatant was collected. After processing the supernatant through a genomic DNA removal column, 70% ethanol was added, and the mixture was transferred to an RNase-Free spin column. After washing and centrifugation, the column was dried, and RNA was eluted with RNase-Free ddH_2O. cDNA synthesis used the FastKing One-Step Kit (Tiangen, Cat# Q712-02). The reaction system contained 4 µL 5× FastKing-RT SuperMix, 0.5 µg total RNA, and made up to 20 µL with RNase-Free ddH_2O. Reverse transcription conditions: 42 °C for 15 min, 95 °C for 3 min. qPCR used ChamQ Universal SYBR qPCR Master Mix (Vazyme, Cat# KR118). The reaction system contained 3 µL cDNA (1:5 diluted), 0.4 µL each of forward and reverse primers (for β-actin and NAMPT, sequences in Table 1), 10 µL 2× SYBR Green mix, made up to 20 µL with ddH_2O. Reaction conditions: 95 °C for 30 s (pre-denaturation), 40 cycles (95 °C for 10 s, 60 °C for 30 s), followed by melt curve analysis. Data were analyzed using the $2^{-\Delta\Delta Ct}$ method to calculate relative expression levels.

2.2.5 Western Blot

Western blot analysis followed standard procedures. Total protein was extracted using Western and IP Cell Lysis Buffer (Beyotime). Tissue samples were homogenized, centrifuged, and the supernatant was collected. Protein concentration was determined using the BCA method (Biosharp kit). Samples were mixed with 5× loading buffer and boiled for 10 min, followed by SDS-PAGE electrophoresis (using FastPAGE precast gels, Tsingke Biotechnology) at a constant voltage of 160 V until the bromophenol blue reached the bottom. Subsequently, proteins were transferred to PVDF membranes (Merck Millipore) at a constant current of 375 mA for 40 min. Membranes were blocked with 5% non-fat milk for 1 h, then incubated with primary antibodies overnight at 4 °C. After washing with TBST, membranes were incubated with HRP-conjugated secondary antibodies for 1 h at room temperature. Finally, signals were detected using ECL substrate (Biosharp) on a chemiluminescence imaging system (Beijing Sage, miniChemi580).

2.2.6 NAD^+/NADH Content Detection

NAD^+ and NADH contents were detected using the water-soluble tetrazolium salt-8 (WST-8) method (Beyotime kit). Tissue samples (20 ± 2 mg) were homogenized in NAD^+/NADH Extraction Buffer, centrifuged, and the supernatant was collected. To distinguish between NAD^+ and NADH, some samples were heated at 60 °C for 30 min to decompose NAD^+, leaving only NADH. For detection, 20 µL of sample was mixed with 90 µL Alcohol Dehydrogenase Working Solution, incubated at 37 °C in the dark for 10 min, then 10 µL Developer was added, incubated for another 30 min, and absorbance was measured at 450 nm. Standard curves were prepared using NADH standards (0–10 µM). Both NAD total and NADH standard curves showed good linearity (NADtotal: $y = 0.1965x - 0.0109$, $R^2 = 0.9966$; NADH: $y = 0.1934x - 0.0308$, $R^2 = 0.9979$). NAD^+ content was calculated as the difference between NAD total and NADH.

2.2.7 Measurement of Secreted IL-6 and IL-8 Levels via ELISA

After cell transfection and grouping treatment (as described in Section 2.2.1), cell culture supernatants were collected and centrifuged at 3000 rpm for 5 min to remove cell debris. All experimental procedures were performed in strict accordance with the instructions of human IL-6 and IL-8 ELISA kits, including serial dilution of standards, sample loading, incubation, and plate washing. Subsequently, enzyme conjugates and chromogenic substrates were added in sequence, and the reaction was terminated. The optical density (OD) of each well was measured at 450 nm with a microplate reader, and the concentrations of IL-6 and IL-8 in the supernatants were calculated from the standard curve.

2.3 Statistical Analysis

Experimental data are expressed as mean ± standard deviation (mean ± SD). Student's *t*-test (for comparison between two groups) or one-way ANOVA (for comparison among multiple groups) was used to assess the significance

of differences between groups. All statistical analyses and graphs preparations were performed using GraphPad Prism (version 8, LLC, Boston, MA, USA). Significant differences in figures are marked as *$p < 0.05$, **$p < 0.01$, ***$p < 0.001$.

For the clinical tissue analyses (n = 4 samples, no control group), no formal statistical comparisons were performed. Data are presented descriptively as individual values or means of technical replicates to illustrate observed trends and variability, consistent with the exploratory nature of this preliminary analysis.

3. Results

3.1 Descriptive Analysis of Lactate, NAD^+/NADH, and NAMPT/SIRT2 Expression in Degenerated Disc Tissue Samples From Four Individuals

To generate hypotheses for subsequent mechanistic studies, tissue samples from 4 patients with degenerative disc disease were analyzed. As shown in Fig. 1A and Table 2 (Ref. [21]), lactate was detected in all four disc tissue samples, with variable levels among individuals (ranging from approximately 700 to 3500 nmol per 50 mg tissue). NAD^+ and NADH contents also varied across the four patient samples (Fig. 1B). Western blot analysis revealed that *NAMPT* and SIRT2 protein expression levels exhibited synchronous trends—samples with higher *NAMPT* expression tended to show higher SIRT2 expression, and vice versa (Fig. 1C). These descriptive observations suggest a potential relationship between *NAMPT* and SIRT2 that may be relevant to disc pathophysiology; however, formal correlation analysis was not performed given the small sample size and absence of a control group. These preliminary findings motivated our subsequent *in vitro* investigations into the functional interaction between *NAMPT*. Lactate was detected in all four disc tissue samples, with variable levels among individuals NAD^+ and NADH contents also varied across the four patient samples (Fig. 1B). Western blot analysis revealed that *NAMPT* and SIRT2 protein expression levels exhibited synchronous trends—samples with higher *NAMPT* expression tended to show higher SIRT2 expression, and vice versa (Fig. 1C and **Supplementary Fig. 1**). These descriptive observations suggest a potential relationship between *NAMPT* and SIRT2 that may be relevant to disc pathophysiology; however, formal correlation analysis was not performed given the small sample size and absence of a control group. These preliminary findings motivated our subsequent *in vitro* investigations into the functional interaction between *NAMPT* and SIRT2.

3.2 Lactate Promotes Senescence of Nucleus Pulposus Cells

NPCs express the specific protein collagen II. Experimental results indicated that the vast majority of the identified cells expressed collagen II. (Fig. 2A), indicating the vast majority of cells and that the phenotype conforms to the characteristics of nucleus pulposus cells. To investigate the senescence-inducing effect of lactate on human nucleus pulposus cells, a blank control group and a lactate treatment group were established. Western blot results showed that, compared with the control group, the overall protein lactylation level was significantly increased in the lactate treatment group, as judged from the representative blots (Fig. 2B). Quantitative analysis further confirmed a 1.20-fold increase relative to the control group (**Supplementary Fig. 2**). Concurrently, results from cellular senescence-associated β-galactosidase staining showed more intense blue staining and an increased number of positive cells in the lactate treatment group, indicating aggravated cellular senescence (Fig. 2C). These results suggest that lactate can increase protein lactylation levels and induce cellular senescence. Furthermore, to assess the SASP, we measured the levels of pro-inflammatory cytokines IL-6 and IL-8 in the culture supernatants by ELISA. Compared with the control group, the LA group exhibited approximately 2.5-fold and 4-fold increases in IL-6 and IL-8 secretion, respectively (both $p < 0.001$; Fig. 2D,E). These results suggest that lactate can increase protein lactylation levels, induce cellular senescence, and promote a pro-inflammatory secretory phenotype.

3.3 Lactate Induces Senescence in Human Nucleus Pulposus Cells by Regulating the p38-MAPK Signaling Pathway

To explore the molecular mechanism by which lactate induces senescence in nucleus pulposus cells, this study examined the phosphorylation level of a key protein in the p38-MAPK signaling pathway and cellular senescence. As shown in Fig. 3A, the expression level of p-p38 protein was significantly increased in the lactate treatment group; however, upon addition of the AMPK activator, p-p38 expression was inhibited. Quantitative analysis revealed a 2.45-fold increase in the LA group and a 1.76-fold increase in the LA+LD group relative to the control (**Supplementary Fig. 3**). Meanwhile, β-galactosidase staining results (Fig. 3B) showed that the lactate-induced cellular senescence was alleviated upon addition of the AMPK activator. These results suggest that lactate may induce senescence of nucleus pulposus cells by activating the p38-MAPK signaling pathway.

3.4 Effect of NAMPT Interference on Lactate Metabolism and NAD^+ Synthesis in Nucleus Pulposus Cells

To verify the regulatory role of *NAMPT* in lactate metabolism and NAD^+ synthesis in nucleus pulposus cells, this study successfully constructed an NPC model with *NAMPT* knockdown (si-*NAMPT*). As shown in Fig. 4A, compared with the empty vector transfection group (siNC), the mRNA expression level of the *NAMPT* gene was significantly decreased in the *NAMPT* interference group (si*NAMPT*), indicating successful model construction. Fur-

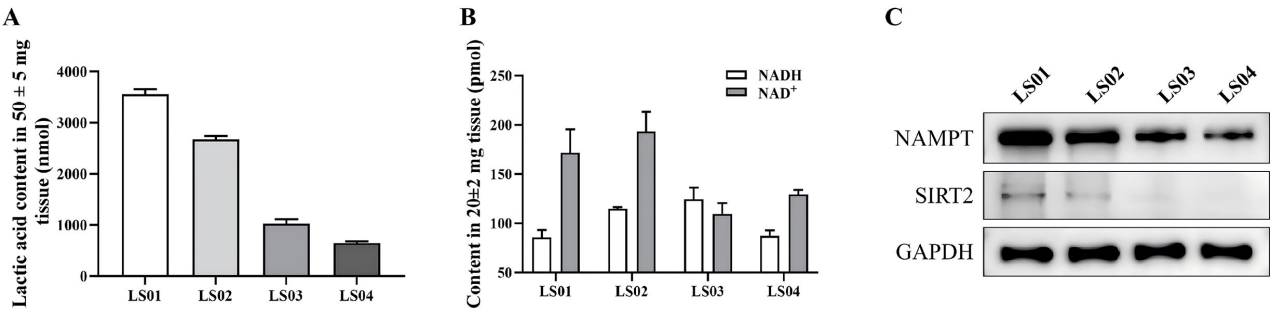

Fig. 1. Descriptive analysis of lactate, NAD^+/NADH, and protein expression in degenerated intervertebral disc tissues from four individual patients. (A) Lactate content in disc tissues of each patient (n = 4 biological samples, each from one patient). Data are presented as mean ± SD of technical duplicates. No statistical comparison was performed due to the lack of a normal control group and the small exploratory sample size. (B) NAD^+ and NADH contents in the same disc tissues (n = 4). Data are shown as mean ± SD of technical replicates. (C) Western blot analysis of SIRT2 and *NAMPT* protein expression in each of the four patient samples. *GAPDH* was used as a loading control. Representative blots from the four individual samples are shown. The observed trends suggest a potential positive correlation between *NAMPT* and SIRT2 expression, but formal correlation analysis was not performed given the limited sample size. These data are presented for descriptive purposes only. The small sample size (n = 4) and lack of normal control tissues preclude any conclusions about disease-associated abnormalities or statistical correlations. Rather, these observations serve as hypothesis-generating findings that informed the design of the subsequent *in vitro* mechanistic experiments. Abbreviation: NAD^+, Nicotinamide adenine dinucleotide; SIRT2, Sirtuin 2; *NAMPT*, Nicotinamide phosphoribosyltransferase; *GAPDH*, Glyceraldehyde-3-phosphate dehydrogenase.

Table 2. Clinical sample information for LDH patients.

Sample ID	Gender	Age (years)	Lumbar JOA total score	Subjective symptoms (Score)	Clinical signs (Score)	Limitation of ADL (Score)
LS01	Female	70	13	1	4	8
LS02	Male	74	13	1	5	7
LS03	Male	56	13	1	3	9
LS04	Female	77	14	2	4	8

Note: LDH, lumbar disc herniation; JOA, Japanese Orthopaedic Association [21]. This study is a preliminary exploratory analysis, including 4 samples to illustrate individual characteristics. These data are presented for descriptive purposes only, illustrating the clinical characteristics of the four individual patients whose samples were used for hypothesis-generating analyses. No control group was included; therefore, no statistical comparisons or inferences about disease associations are made.

ther detection revealed that after interfering with *NAMPT* expression, both intracellular lactate (Fig. 4B) and NAD^+ (Fig. 4C) contents were significantly decreased compared to the siNC group. Notably, treatment with a SIRT2-specific activator (SIRT2o) following *NAMPT* interference partially restored intracellular lactate content (Fig. 4B), but NAD^+ content showed no significant change (Fig. 4C). These results suggest that *NAMPT* may influence lactate metabolism in nucleus pulposus cells by regulating SIRT2 activity.

3.5 Overexpression of NAMPT Induces Senescence in Human Nucleus Pulposus Cells by Regulating Lactate Metabolism

To verify the regulatory roles of *NAMPT* and lactate in the senescence of nucleus pulposus cells, this study constructed a human nucleus pulposus cell model with *NAMPT* overexpression. As shown in Fig. 5A, compared with the blank control group (oeNC), the *NAMPT* mRNA level in the overexpression group (oe*NAMPT*) was significantly increased, indicating successful model construction. β-galactosidase staining results (Fig. 5C) showed an increased number of senescence-positive cells in the oe group compared to the oeNC group. Concurrently, intracellular lactate content detection (Fig. 5B) revealed a significant increase in lactate levels in the oe group, suggesting that *NAMPT* overexpression may lead to lactate accumulation. To investigate the role of lactate in *NAMPT*-induced cellular senescence, a lactate inhibitor and a SIRT2 inhibitor were added individually based on overexpression. Results showed that, compared with the oe group, both the lactate inhibitor and the SIRT2 inhibitor effectively reduced intracellular lactate levels (Fig. 5B) and significantly decreased the number of β-galactosidase-positive cells (Fig.

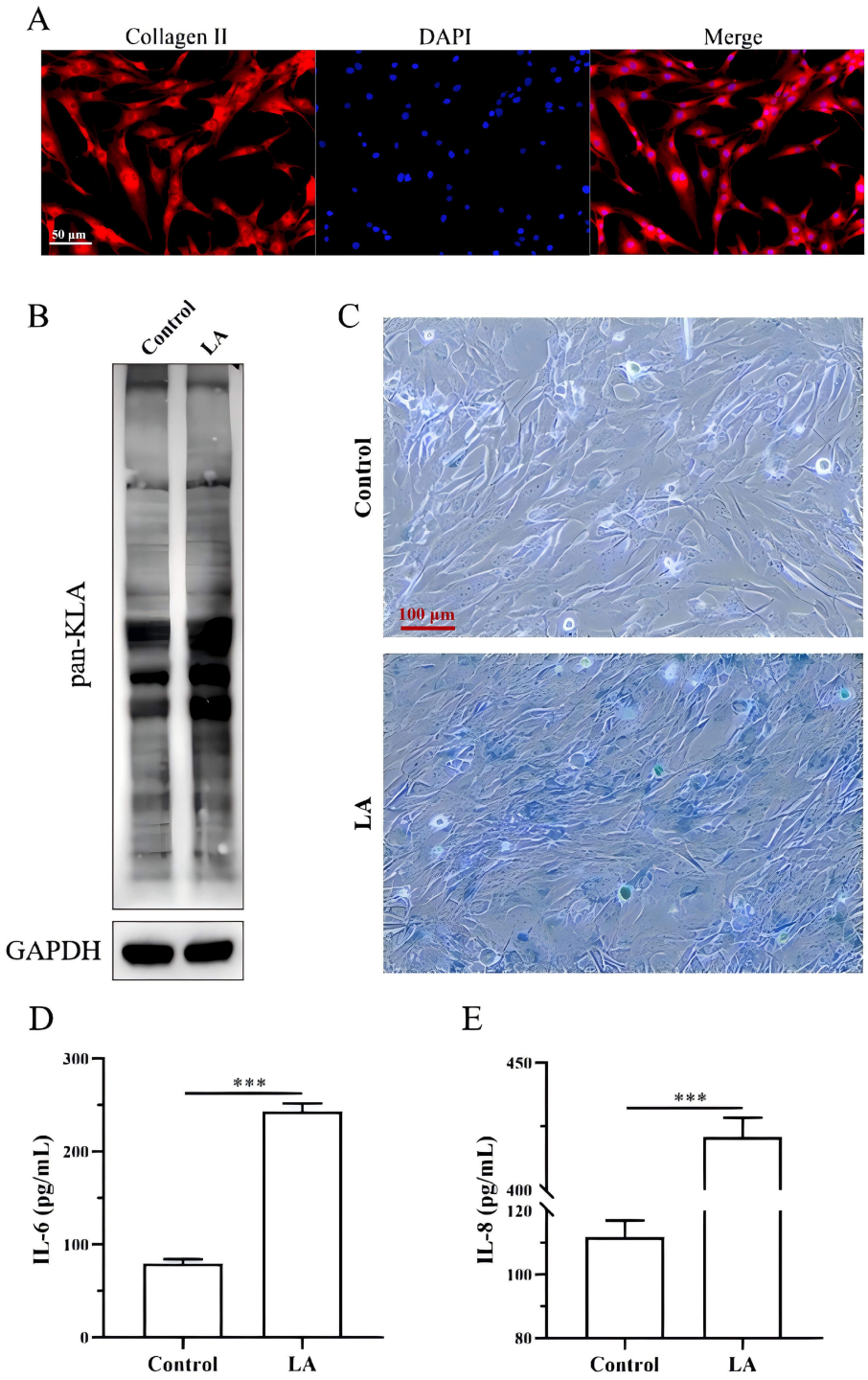

Fig. 2. Effect of lactate on senescence of nucleus pulposus cells (NPCs). (A) Identification of nucleus pulposus cells using Collagen II immunofluorescence staining (Magnification = 200×); Scale bar = 50μm. (B) Detection of global protein lactylation levels (pan-KLA) in each group by Western blot, GAPDH was used as an internal control. (C) Detection of cellular senescence using β-galactosidase staining, blue-stained areas indicate senescence-positive cells. Scale bar = 100μm. ELISA quantification of (D) IL-6 and (E) IL-8 secretion in the culture supernatants of Control and lactate-treated (LA) groups. Data are presented as mean ± SD from three independent experiments. ***$p < 0.001$ vs. Control group.

5C). These results suggest that *NAMPT* functionally interacts with SIRT2 to influence lactate metabolism and cellular senescence, although the precise molecular details (e.g., SIRT2 protein levels, enzymatic activity, or substrate acetylation) were not directly investigated in this study.

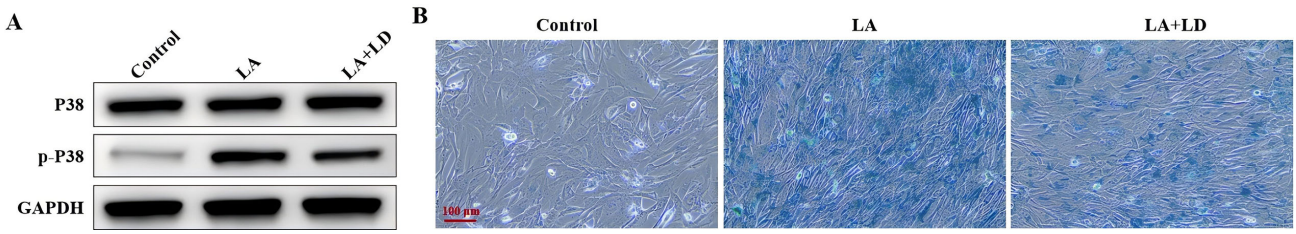

Fig. 3. Effect of lactate on the p38-MAPK signaling pathway and senescence in human nucleus pulposus cells. (A) Expression levels of p-p38 protein in each group, with GAPDH used as an internal control. Data are presented as mean ± SD from three biological replicates. (B) Detection of cellular senescence by β-galactosidase staining. Representative images from three independent experiments are shown. Scale bar = 100 μm. Blue-stained cells were counted as senescence-positive.

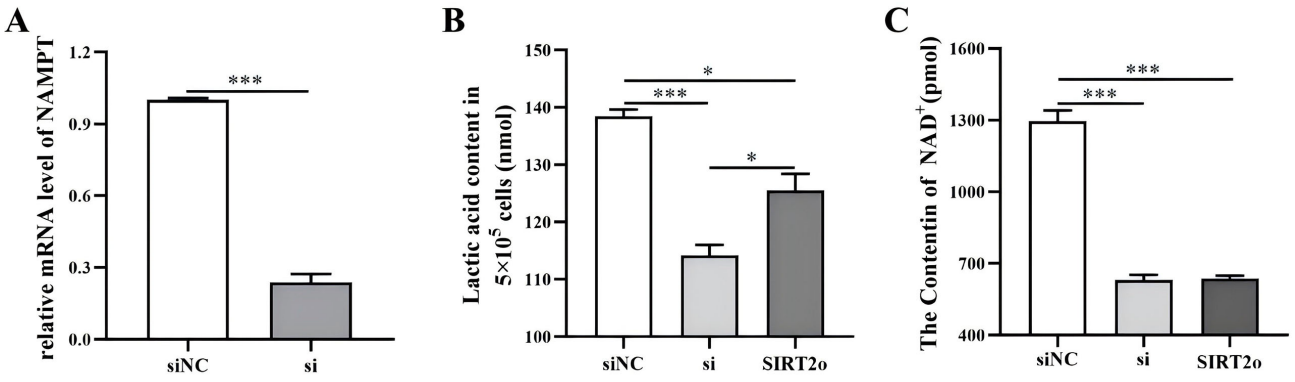

Fig. 4. Effects of *NAMPT* interference on lactate and NAD^+ contents in nucleus pulposus cells. (A) Relative mRNA expression of *NAMPT* in each group; the si group showed a significant decrease compared with the siNC group. (B) Intracellular lactate content in each group; the si group was significantly lower than the siNC group, and the si+SIRT2o (SIRT2 activator) group showed a partial recovery compared with the si group. (C) NAD^+ content in each group; the si group was significantly lower than the siNC group, but no significant difference was observed between the si+SIRT2o and si groups. All data are presented as mean ± SD from three independent experiments. Statistical comparisons were performed using one-way ANOVA followed by Tukey's post hoc test. $*p < 0.05$, $***p < 0.001$.

4. Discussion

In a preliminary analysis of four degenerated disc tissue samples, lactate was detected at variable levels, and *NAMPT* and SIRT2 protein expression showed synchronous trends. These descriptive observations suggested a potential relationship among these factors that warranted further investigation. To verify this association at the cellular level and probe its underlying mechanisms, we selected NPCs for *in vitro* experiments [9,22]. These cells are the primary effectors responsible for producing and maintaining the disc's core extracellular matrix components, including type II collagen [23]. *In vitro* experiments confirmed that lactate treatment not only significantly elevated the overall protein lactylation level in NPCs but also exacerbated cellular senescence by activating the p38-MAPK signaling pathway. Mechanistically, *NAMPT* is a key upstream node regulating this process: interfering with *NAMPT* expression reduced intracellular lactate and NAD^+ levels, an effect that could be partially reversed by SIRT2 activation; conversely, overexpressing *NAMPT* induced lactate accumulation and promoted senescence, a process antagonized by a lactate inhibitor or SIRT2 inhibitor. In summary, the results of this study reveal a molecular mechanism regulating NPC senescence: *NAMPT* influences lactate metabolism by affecting SIRT2 activity, thereby regulating the p38-MAPK pathway and impacting the senescence process.

It should be noted that latrepirdine, though originally developed as a neuroprotective agent, multiple peer-reviewed papers have verified its reliable AMPK-activating property. Prehn demonstrated that latrepirdine potently elevates p-AMPKα at nanomolar concentrations independent of its classic neuroreceptor-blocking activity. Also, Coughlan et al. [24] directly applied latrepirdine as a canonical AMPK activator for *in vivo* animal research, and this application has been widely accepted. Metformin and AICAR were abandoned due to poor performance in NPCs. NPCs express low levels of OCT transporters required for metformin uptake; AICAR needs intracellular metabolic conversion and shows unstable efficacy in highly glycolytic

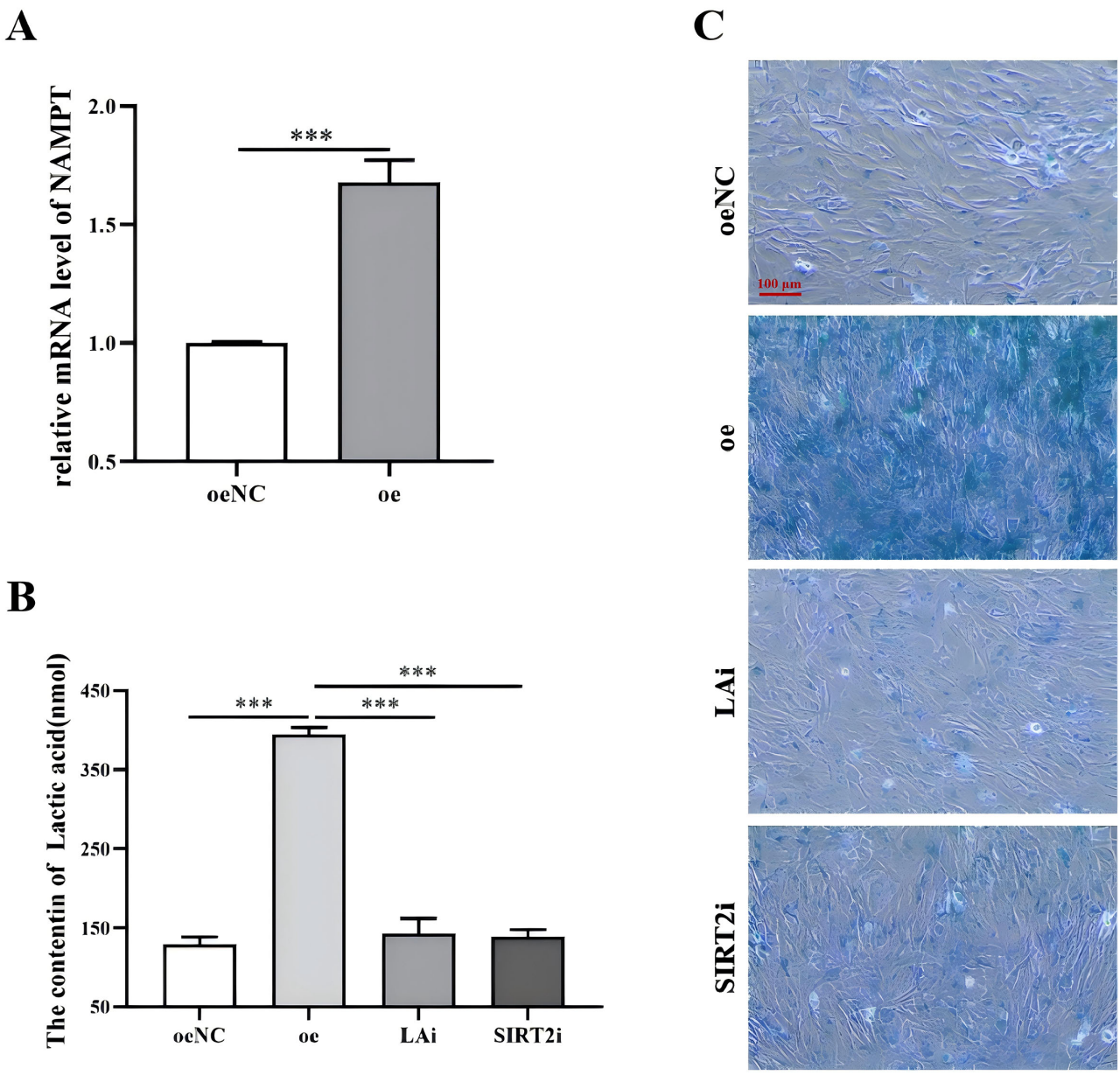

Fig. 5. Effects of NAMPT overexpression on senescence and lactate content in nucleus pulposus cells. (A) Relative mRNA expression of *NAMPT* in each group; the oe group showed a significant increase compared with the oeNC group. (B) Intracellular lactate content in each group; the oe group was significantly higher than the oeNC group, and both the LAi and SIRT2i groups were significantly lower than the oe group. (C) Detection of cellular senescence by β-galactosidase staining; blue particles indicate senescence-positive cells. All data are presented as mean ± SD from three independent experiments. Statistical comparisons were performed using one-way ANOVA followed by Tukey's post hoc test. ***$p < 0.001$. Scale bar in (C) = 100 μm.

NPCs. By contrast, lipophilic latrepirdine enters cells without requiring transporters or intracellular activation. At the concentration used (100 nM), latrepirdine has no cytotoxicity and sustains AMPK activation for over 24 h, fitting our long-term cellular senescence intervention. Besides, it effectively mediates the crosstalk between AMPK and p38-MAPK, matching our experimental design.

As an avascular tissue, the intervertebral disc primarily relies on anaerobic glycolysis for energy [25]. This metabolic pathway generates ATP while reducing NAD^+ to NADH; to sustain glycolysis, LDH reduces pyruvate to lactate, regenerating NAD^+ in this process, thus establishing a dynamic coupling between lactate production and the NAD^+/NADH ratio [26]. Under physiological conditions, the production, transport, and clearance of lactate maintain a dynamic balance, crucial for regulating intracellular pH and maintaining homeostasis within the intervertebral disc [17]. However, during disc degeneration, end-

plate calcification impedes nutrient supply, along with disrupted intracellular glucose metabolism, collectively disrupting lactate metabolic balance and ultimately leading to its pathological accumulation in degenerated tissues [27]. Notably, this study found that degenerated disc tissues not only exhibited significant lactate accumulation but also showed a concurrent increase in the NAD^+/NADH ratio in samples with higher lactate levels, suggesting that lactate metabolic disorder might disrupt intracellular redox homeostasis. Previous studies [14,28,29] have indicated that an elevated NAD^+/NADH ratio can further activate downstream stress signaling pathways, thereby promoting senescence and apoptosis of NPCs—which are core cellular events in IDD [28]. Furthermore, as reported in the literature, nuclear-localized MKP1 dephosphorylates p38 -MAPK, reducing LKB1 phosphorylation and its nuclear export, thereby inhibiting the activation of AMPKα in the cytoplasm [30]. This mechanism suggests that the inactivation of AMPKα might be closely related to the regulation of the p38-MAPK pathway. Therefore, to verify the role of p38-MAPK in lactate-induced NPC senescence, this study employed an AMPKα activator in intervention experiments. Mechanistically, this study confirmed that lactate treatment significantly activated the p38-MAPK signal, manifested by upregulated p-p38 protein expression, while activating the AMPKα pathway could inhibit p-p38 expression, thereby alleviating lactate-induced cellular senescence. This result is consistent with previous reports: p38-MAPK signaling is activated in both the nucleus pulposus tissue of IDD patients and lipopolysaccharide-induced NPCs, and inhibiting JNK/p38-MAPK signaling promotes NPC proliferation [31]. In conclusion, this study suggests that in degenerated discs, lactate accumulation might alter the NAD^+/NADH balance and activate the p38-MAPK pathway, thereby driving NPC senescence and ultimately participating in the pathological progression of IDD.

NAMPT, as the rate-limiting enzyme in NAD^+ biosynthesis, is crucial for maintaining cellular metabolic homeostasis [32]. The literature reports that adipocyte-derived exosomes can deliver *NAMPT* to senescent cells, elevating NAD^+ levels and activating SIRT1, thereby alleviating intervertebral disc degeneration [14]. In this study, interfering with *NAMPT* expression indeed led to a synchronous decrease in intracellular NAD^+ and lactate levels, suggesting that *NAMPT* regulates both metabolic pathways. Notably, inhibiting *NAMPT* while activating SIRT2 only reversed the decrease in lactate levels, with no significant effect on NAD^+ content. This indicates that *NAMPT*'s regulation of lactate is likely mediated through SIRT2 and may be independent of its classical role in NAD^+ synthesis. This finding aligns with the known function of SIRT2 as an NAD^+-dependent deacetylase capable of regulating the activity of glycolytic enzymes (such as LDHA) [16]; we speculate that SIRT2 activators might specifically restore its regulatory effect on lactate metabolism by enhancing the enzyme's efficiency in utilizing the limited NAD^+ pool. Further studies confirmed that overexpressing *NAMPT* led to lactate accumulation and induced cellular senescence, which were effects reversed by either a lactate inhibitor or a SIRT2 inhibitor. Combined with literature indicating that SIRT2 expression is downregulated in degenerated discs and that its overexpression can alleviate oxidative stress and cellular senescence by inhibiting the p53/p21 pathway [9], this study suggests that in intervertebral disc degeneration, *NAMPT* might influence lactate metabolism through SIRT2, thereby driving a p38-MAPK-dependent senescence program. In summary, the *NAMPT*/SIRT2/lactate axis is confirmed in this study as a key molecular mechanism regulating nucleus pulposus cell senescence and intervertebral disc degeneration.

This study has certain limitations. First, the experiments were based solely on *in vitro* cell models, which cannot fully simulate the complex systemic environment *in vivo*. Notably, *NAMPT* in mammals exists in two forms: intracellular (i*NAMPT*) and extracellular (e*NAMPT*), which may differ in function and regulatory mechanisms [33,34]. Future studies utilizing animal models are needed to further clarify its specific role in intervertebral disc degeneration. Second, this study focused on the *NAMPT*/SIRT2/lactate axis and did not extend to key molecules downstream in extracellular matrix degradation, such as MMP-3, MMP-13, ADAMTS-4/5, which are known targets regulated by *NAMPT* or lactate [35,36]. Despite these limitations, this study provides an important theoretical basis for elucidating the metabolic mechanisms of intervertebral disc degeneration and exploring potential therapeutic targets.

Endplate dysfunction and subsequent nutrient supply failure represent primary upstream events that drive lactate accumulation in disc degeneration. However, we propose that targeting the *NAMPT*/SIRT2 axis is not a "locking the stable door after the horse has bolted" strategy, but rather an intervention aimed at interrupting a self-amplifying vicious cycle. Once endplate impairment initiates lactate accumulation, lactate not only serves as a metabolic waste but also actively promotes nucleus pulposus cell senescence via the p38-MAPK pathway and induces a pro-catabolic, pro-inflammatory secretory phenotype, which in turn may further aggravate endplate degeneration and metabolic dysregulation. Thus, even if the original endplate pathology cannot be fully reversed, blocking the downstream effector machinery—namely the *NAMPT*/SIRT2/lactate signaling node—could halt or slow the progression of this feed-forward loop. Moreover, our data demonstrate that modulating *NAMPT* or SIRT2 activity significantly alters intracellular lactate levels and the NAD^+/NADH ratio (Figs. 4,5), indicating that this axis has the capacity to reshape cellular metabolic homeostasis independently of upstream endplate status. From a translational perspective, while complete restoration of endplate function remains challenging, pharmacologically targeting *NAMPT* or SIRT2 (e.g.,

with small-molecule activators or inhibitors) may offer a disease-modifying approach, particularly in early-to-mid-stage degeneration where some endplate transport capacity persists, or as part of combination regimens that include therapies aimed at improving nutrient supply. Therefore, our findings do not claim to cure the primary endplate failure but rather provide a rationale for breaking the metabolic-senescence vicious cycle, a strategy that has proven successful in other chronic degenerative diseases (e.g., targeting downstream pathways in diabetes despite persistent insulin resistance).

5. Limitations

Several limitations of this study should be acknowledged. First, the clinical tissue analysis included only a small number of degenerated disc samples (n = 4) and lacked normal control tissues. Therefore, our findings regarding lactate, NAD^+/NADH, *NAMPT*, and SIRT2 expression are descriptive and hypothesis-generating rather than definitive. The absence of normal controls precludes any conclusion about "abnormality" of the measured parameters. Larger cohorts with healthy controls are needed to validate the observed trends.

Second, this research is primarily based on *in vitro* cultured human NPCs. While the *in vitro* experiments provide mechanistic insights, they cannot fully recapitulate the complex *in vivo* microenvironment of the intervertebral disc, particularly the critical role of vertebral endplate integrity in regulating nutrient supply and waste product clearance. The accumulation of lactate in degenerated discs is closely linked to endplate dysfunction; however, our current model does not allow us to dissect how endplate failure interacts with the *NAMPT*/SIRT2/lactate axis over time. Therefore, future studies using animal models of intervertebral disc degeneration (e.g., needle puncture or endplate injury models) are essential to validate the *in vivo* relevance of this signaling axis and to assess the therapeutic window for targeting *NAMPT* or SIRT2 under conditions of established endplate compromise. Moreover, all *in vitro* experiments were performed under normoxic conditions, whereas the intervertebral disc is physiologically hypoxic. It is possible that the *NAMPT*/SIRT2/lactate axis operates differently under more physiological oxygen tension.

Third, we did not directly measure SIRT2 protein expression levels, enzymatic activity, or the acetylation status of its classic downstream substrates (e.g., α-tubulin). Our conclusion that *NAMPT* regulates lactate metabolism in a SIRT2-dependent manner is based primarily on pharmacological activator/inhibitor studies, which support a functional interaction but do not elucidate the precise biochemical mechanism (e.g., whether *NAMPT* affects SIRT2 expression, post-translational modification, or catalytic efficiency). Future studies employing SIRT2-specific genetic manipulations (knockdown or overexpression) are required to establish direct causality.

Fourth, the study focuses on the *NAMPT*/SIRT2/lactate/p38-MAPK pathway but does not extend to downstream catabolic effectors such as matrix metalloproteinases (MMP-3, MMP-13), aggrecanases (ADAMTS-4/5), or specific SASP factors, which are known to be regulated by lactate or *NAMPT* in other cell types. Whether the observed cellular senescence directly translates into matrix degradation and functional disc deterioration remains to be further elucidated. Furthermore, while we used an AMPK activator to indirectly modulate p38 phosphorylation, we did not employ a direct p38-specific inhibitor (e.g., SB203580) to confirm the necessity of the p38-MAPK pathway. This should be addressed in future mechanistic studies.

Fifth, *NAMPT* in mammals exists in both intracellular (i*NAMPT*) and extracellular (e*NAMPT*) forms, which may exert distinct or even opposing functions in metabolism and senescence. Our experimental manipulations (siRNA and overexpression plasmid) primarily target total *NAMPT* expression and do not distinguish between these two pools. The relative contribution of i*NAMPT* versus e*NAMPT* to the regulation of SIRT2 activity and lactate production in NPCs requires additional investigation.

Finally, regarding the translational implications, while targeting *NAMPT* or SIRT2 may offer a potential disease-modifying strategy, it is unlikely to reverse pre-existing endplate calcification or restore nutrient transport. Thus, such an approach should be viewed as a complementary intervention aimed at disrupting the self-amplifying cycle of metabolic stress and cellular senescence, rather than as a standalone cure for the primary cause of disc degeneration. Future studies combining *NAMPT*/SIRT2 modulation with strategies to improve endplate function or nutritional supply may yield more robust therapeutic benefits.

6. Conclusion

This study identifies the *NAMPT*/SIRT2/lactate signaling axis as a candidate regulatory pathway in nucleus pulposus cell senescence. *In vitro* mechanistic studies revealed that *NAMPT* modulates lactate metabolism in a SIRT2-dependent manner, subsequently activating the p38-MAPK pathway and driving cellular senescence. While the clinical relevance of these findings requires validation in larger patient cohorts with appropriate controls, the descriptive observations from four degenerated disc samples provided the initial rationale for this investigation. This work provides a foundation for future studies examining the metabolic-senescence axis in intervertebral disc degeneration. Further studies are needed to determine whether this involves changes in SIRT2 expression, activity, or downstream deacetylation targets. This finding not only reveals a novel metabolic-senescence regulatory pathway but also provides a potential therapeutic strategy for intervening in IDD, particularly in the context of interrupting the lactate-driven vicious cycle of cellular senescence. Given the mul-

tifactorial nature of IDD and the upstream role of endplate dysfunction, such an approach is best viewed as a complementary intervention rather than a standalone cure for the primary cause.

Availability of Data and Materials

The datasets and raw data used and analyzed during the current study are available from the corresponding author on reasonable request.

Author Contributions

WZ conceived the project, designed the research, and contributed to the manuscript preparation. LM and HG performed the research. XZ, HT, and WL performed the data analysis. WZ and CL contributed to data acquisition, the initial manuscript, and manuscript revision. All authors contributed to editorial changes in the manuscript. All authors read and approved the final manuscript. All authors have participated sufficiently in the work and agreed to be accountable for all aspects of the work.

Ethics Approval and Consent to Participate

This study was approved by the ethics committee of the Third Affiliated Hospital of Guangzhou University of Chinese Medicine (approved No. YJ-KY-20250307-007). We certify that the study was performed in accordance with the 1964 declaration of HELSINKI and later amendments. Written informed consent to participate in this study was provided by the patients or their families/legal guardians.

Acknowledgment

We would like to express our sincere gratitude to all the clinical volunteers who participated in this study. Their invaluable contribution in providing the clinical samples was essential for the successful completion of this research. We deeply appreciate their time, cooperation, and commitment, which made this work possible.

Funding

This research was funded by Research Project of Guangdong Provincial Bureau of Traditional Chinese Medicine (20254086).

Conflicts of Interest

The authors declare no conflicts of interest.

Declaration of AI and AI-Assisted Technologies in the Writing Process

During the preparation of this work the authors used Deepseek-R1 in order to check spelling and grammar. After using this tool, the authors reviewed and edited the content as needed and take full responsibility for the content of the publication.

Supplementary Material

Supplementary material associated with this article can be found, in the online version, at https://doi.org/10.31083/FBL51724.

References

[1] Knezevic NN, Candido KD, Vlaeyen JWS, Van Zundert J, Cohen SP. Low back pain. Lancet (London, England), 2021: 398: 78–92. https://doi.org/10.1016/S0140-6736(21)00733-9

[2] Mohd Isa IL, Teoh SL, Mohd Nor NH, Mokhtar SA. Discogenic Low Back Pain: Anatomy, Pathophysiology and Treatments of Intervertebral Disc Degeneration. International Journal of Molecular Sciences. 2022; 24: 208. https://doi.org/10.3390/ijms24010208

[3] Jiang L, Zhang X, Zheng X, Ru A, Ni X, Wu Y, et al. Apoptosis, senescence, and autophagy in rat nucleus pulposus cells: Implications for diabetic intervertebral disc degeneration. Journal of Orthopaedic Research: Official Publication of the Orthopaedic Research Society. 2013; 31: 692–702. https://doi.org/10.1002/jor.22289

[4] Zhao CQ, Wang LM, Jiang LS, Dai LY. The cell biology of intervertebral disc aging and degeneration. Ageing Research Reviews. 2007; 6: 247–261. https://doi.org/10.1016/j.arr.2007.08.001

[5] Adams MA, Roughley PJ. What is intervertebral disc degeneration, and what causes it? Spine. 2006; 31: 2151–2161. https://doi.org/10.1097/01.brs.0000231761.73859.2c

[6] Brooks GA. The Science and Translation of Lactate Shuttle Theory. Cell Metabolism. 2018; 27: 757–785. https://doi.org/10.1016/j.cmet.2018.03.008

[7] Wu W, Zhang X, Hu X, Wang X, Sun L, Zheng X, et al. Lactate down-regulates matrix systhesis and promotes apoptosis and autophagy in rat nucleus pulposus cells. Journal of Orthopaedic Research: Official Publication of the Orthopaedic Research Society. 2014; 32: 253–261. https://doi.org/10.1002/jor.22503

[8] Zhang Y, Liu L, Qi Y, Lou J, Chen Y, Liu C, et al. Lactic acid promotes nucleus pulposus cell senescence and corresponding intervertebral disc degeneration via interacting with Akt. Cellular and, Molecular Life Sciences: CMLS. 2024; 81: 24. https://doi.org/10.1007/s00018-023-05094-y

[9] Yang M, Peng Y, Liu W, Zhou M, Meng Q, Yuan C. Sirtuin 2 expression suppresses oxidative stress and senescence of nucleus pulposus cells through inhibition of the p53/p21 pathway. Biochemical and Biophysical Research Communications. 2019; 513: 616–622. https://doi.org/10.1016/j.bbrc.2019.03.200

[10] Zhong F, Cen S, Long C, Teng L, Zhong G. SIRT2 Alleviates Inflammatory Response, Apoptosis, and ECM Degradation in Osteoarthritic Chondrocytes by Stabilizing PCK1. Discovery Medicine. 2024; 36: 2046–2054. https://doi.org/10.24976/Discov.Med.202436189.188

[11] Gagarina V, Gabay O, Dvir-Ginzberg M, Lee EJ, Brady JK, Quon MJ, et al. SirT1 enhances survival of human osteoarthritic chondrocytes by repressing protein tyrosine phosphatase 1B and activating the insulin-like growth factor receptor pathway. Arthritis and Rheumatism. 2010; 62: 1383–1392. https://doi.org/10.1002/art.27369

[12] Hassan B, Baroukh B, Llorens A, Lesieur J, Ribbes S, Chaussain C, et al. NAMPT expression in osteoblasts controls osteoclast recruitment in alveolar bone remodeling. Journal of Cellular Physiology. 2018; 233: 7402–7414. https://doi.org/10.1002/jcp.26584

[13] Laiguillon MC, Houard X, Bougault C, Gosset M, Nourissat G, Sautet A, et al. Expression and function of visfatin (Nampt), an adipokine-enzyme involved in inflammatory pathways of

osteoarthritis. Arthritis Research & Therapy. 2014; 16: R38. https://doi.org/10.1186/ar4467

[14] Sun Y, Li X, Yang X, Chen B, Zhang W. Small Extracellular Vesicles Derived from Adipocytes Attenuate Intervertebral Disc Degeneration in Rats by Rejuvenating Senescent Nucleus Pulposus Cells and Endplate Cells by Delivering Exogenous NAMPT. Oxidative Medicine and Cellular Longevity. 2021; 2021: 9955448. https://doi.org/10.1155/2021/9955448

[15] Miranda ER, Varshney P, Mazo CE, Shadiow J, Ludlow AT, Haus JM. Loss of NAMPT and SIRT2 but not SIRT1 attenuate GLO1 expression and activity in human skeletal muscle. Redox Biology. 2024; 75: 103300. https://doi.org/10.1016/j.redox.2024.103300

[16] Liu K, Wei H, Nong W, Peng H, Li Y, Lei X, et al. Nampt/SIRT2/LDHA pathway-mediated lactate production regulates follicular dysplasia in polycystic ovary syndrome. Free Radical Biology & Medicine. 2024; 225: 776–793. https://doi.org/10.1016/j.freeradbiomed.2024.10.312

[17] Silagi ES, Novais EJ, Bisetto S, Telonis AG, Snuggs J, Le Maitre CL, et al. Lactate Efflux From Intervertebral Disc Cells Is Required for Maintenance of Spine Health. Journal of Bone and Mineral Research: the Official Journal of the American Society for Bone and Mineral Research. 2020; 35: 550–570. https://doi.org/10.1002/jbmr.3908

[18] Malandrino A, Noailly J, Lacroix D. The effect of sustained compression on oxygen metabolic transport in the intervertebral disc decreases with degenerative changes. PLoS Computational Biology. 2011; 7: e1002112. https://doi.org/10.1371/journal.pcbi.1002112

[19] Liu Y, Yang J, Wang Z, Fu J, Liu H, Lu Z, et al. Lactate and lactylation in intervertebral disc degeneration. Frontiers in Molecular Biosciences. 2025; 12: 1685975. https://doi.org/10.3389/fmolb.2025.1685975

[20] Zhang Y, Huang Z, Han W, Wu J, Li S, Qin T, et al. Glutamine suppresses senescence and promotes autophagy through glycolysis inhibition-mediated AMPKα lactylation in intervertebral disc degeneration. Communications Biology. 2024; 7: 325. https://doi.org/10.1038/s42003-024-06000-3

[21] Clinical Outcomes Committee of the Japanese Orthopaedic Association, Subcommittee on Evaluation of Back Pain and Cervical Myelopathy, Subcommittee on Low Back Pain and Cervical Myelopathy Evaluation of the Clinical Outcome Committe of the Japanese Orthopaedic Association, Fukui M, Chiba K, Kawakami M, et al.JOA back pain evaluation questionnaire: initial report. Journal of Orthopaedic Science: Official Journal of the Japanese Orthopaedic Association. 2007; 12: 443–450. https://doi.org/10.1007/s00776-007-1162-x

[22] Basatvat S, Bach FC, Barcellona MN, Binch AL, Buckley CT, Bueno B, et al. Harmonization and standardization of nucleus pulposus cell extraction and culture methods. JOR Spine. 2023; 6: e1238. https://doi.org/10.1002/jsp2.1238

[23] Liao Z, Luo R, Li G, Song Y, Zhan S, Zhao K, et al. Exosomes from mesenchymal stem cells modulate endoplasmic reticulum stress to protect against nucleus pulposus cell death and ameliorate intervertebral disc degeneration in vivo. Theranostics. 2019; 9: 4084–4100. https://doi.org/10.7150/thno.33638

[24] Coughlan KS, Mitchem MR, Hogg MC, Prehn JHM. "Preconditioning" with latrepirdine, an adenosine 5'-monophosphate-activated protein kinase activator, delays amyotrophic lateral sclerosis progression in SOD1(G93A) mice. Neurobiology of Aging. 2015; 36: 1140–1150. https://doi.org/10.1016/j.neurobiolaging.2014.09.022

[25] Song C, Hu P, Peng R, Li F, Fang Z, Xu Y. Bioenergetic dysfunction in the pathogenesis of intervertebral disc degeneration. Pharmacological Research. 2024; 202: 107119. https://doi.org/10.1016/j.phrs.2024.107119

[26] Luengo A, Li Z, Gui DY, Sullivan LB, Zagorulya M, Do BT, et al. Increased demand for NAD^+ relative to ATP drives aerobic glycolysis. Molecular Cell. 2021; 81: 691–707.e6. https://doi.org/10.1016/j.molcel.2020.12.012

[27] Kirnaz S, Capadona C, Wong T, Goldberg JL, Medary B, Sommer F, et al. Fundamentals of Intervertebral Disc Degeneration. World Neurosurgery. 2022; 157: 264–273. https://doi.org/10.1016/j.wneu.2021.09.066

[28] Jiang L, Cao L, Ma Y, Chen Q, Liang Y, Yuan F, et al. TIGAR mediates the inhibitory role of hypoxia on ROS production and apoptosis in rat nucleus pulposus cells. Osteoarthritis Cartilage. 2018; 26: 138-148.https://doi.org/10.1016/j.joca.2017.10.007

[29] Wang D, Hu Z, Hao J, He B, Gan Q, Zhong X, et al. SIRT1 inhibits apoptosis of degenerative human disc nucleus pulposus cells through activation of Akt pathway. Age (Dordrecht, Netherlands). 2013; 35: 1741–1753. https://doi.org/10.1007/s11357-012-9474-y

[30] Niture S, Mooers BHM, Wu DH, Hart M, Jaboin J, Seneviratne D. Dual-specificity protein phosphatase 1: A potential therapeutic target in cancer. iScience. 2025; 28: 113706. https://doi.org/10.1016/j.isci.2025.113706

[31] Zhong H, Guo L, Guo W, Liu F, Zheng B, Zhang S, et al. Activation of JNK/p38 MAPK Signaling Pathway by lncRNA DGCR5 Promotes Nucleus Pulposus Cell Degeneration and Pyroptosis in Intervertebral Disk Degeneration. Neurosurgery. 2025; 97: 752–761. https://doi.org/10.1227/neu.0000000000003406

[32] Imai S, Yoshino J. The importance of NAMPT/NAD/SIRT1 in the systemic regulation of metabolism and ageing. Diabetes, Obesity & Metabolism. 2013; 15: 26–33. https://doi.org/10.1111/dom.12171

[33] Park JW, Roh E, Kang GM, Gil SY, Kim HK, Lee CH, et al. Circulating blood eNAMPT drives the circadian rhythms in locomotor activity and energy expenditure. Nature Communications. 2023; 14: 1994. https://doi.org/10.1038/s41467-023-37517-6

[34] Revollo JR, Körner A, Mills KF, Satoh A, Wang T, Garten A, et al. Nampt/PBEF/Visfatin regulates insulin secretion in beta cells as a systemic NAD biosynthetic enzyme. Cell Metabolism. 2007; 6: 363–375. https://doi.org/10.1016/j.cmet.2007.09.003

[35] Huang YF, Wang G, Ding L, Bai ZR, Leng Y, Tian JW, et al. Lactate-upregulated NADPH-dependent NOX4 expression via HCAR1/PI3K pathway contributes to ROS-induced osteoarthritis chondrocyte damage. Redox Biology. 2023; 67: 102867. https://doi.org/10.1016/j.redox.2023.102867

[36] Shi C, Wu H, Du D, Im HJ, Zhang Y, Hu B, et al. Nicotinamide Phosphoribosyltransferase Inhibitor APO866 Prevents IL-1β-Induced Human Nucleus Pulposus Cell Degeneration via Autophagy. Cellular Physiology and Biochemistry: International Journal of Experimental Cellular Physiology, Biochemistry, and Pharmacology. 2018; 49: 2463–2482. https://doi.org/10.1159/000493843